STUDY ON OTFS MODULATION & CHANNEL ESTIMATION TECHNIQUES

A Project Report

submitted by

K R SRINIVAS [EE18B136]

in partial fulfilment of the requirements
for the award of the degree of

DUAL DEGREE

DEPARTMENT OF ELECTRICAL ENGINEERING
INDIAN INSTITUTE OF TECHNOLOGY MADRAS.

MAY 2023

THESIS CERTIFICATE

This is to certify that the thesis titled **STUDY ON OTFS MODULATION & CHANNEL ESTIMATION TECHNIQUES**, submitted by **K R SRINIVAS**, to the Indian Institute of Technology Madras, for the award of the degree of **DUAL DEGREE**, is a bona fide record of the research work done by him under my supervision. The contents of this thesis, in full or in parts, have not been submitted to any other Institute or University for the award of any degree or diploma.

Prof. R David Koilpillai
Research Guide
Professor
Dept. of Electrical Engineering
IIT Madras, 600 036

Place: Chennai

Date: 12.05.2023

ACKNOWLEDGEMENTS

I would like to thank my guide, Dr. R David Koilpillai for their continuous and consistent efforts in guiding me throughout the project. Their guidance, support and vast knowledge in the field helped me in solving problems that routinely came up during the course of the project. I am forever grateful to have been able to work on this project, under both of them. I would like to thank Mr. Narendra Deconda for helping me at several instances throughout this project.

I would also like to thank IIT Madras for the knowledge, opportunities and experience that it has provided me over the last five years. This institute greatly contributed to my overall development as an engineer, as well as to my personal growth.

ABSTRACT

The goal of this project is to study the recently proposed radio access technology, a new two-dimensional modulation technique called Orthogonal Time–Frequency Space Modulation, designed in the delay-Doppler domain, suited very well for high-mobility environments.

The study will assess the current limitations of OFDM when dealing with a high-mobility environment, present an overview of delay-Doppler domain representation of the wireless channels, and the fundamentals of OTFS modulation.

Frequency spreading due to high-Doppler shift leads to inter-carrier interference (ICI) in Orthogonal Frequency Division Multiplexing (OFDM). As a result, channel estimation and, consequently, data detection performance are poor. The resilience of OTFS modulation to high-Doppler shifts and slow variability and the sparse nature of wireless channels in the delay-Doppler domain allows us to simplify channel estimation. We will look at the state-of-the-art approaches in delay-Doppler domain channel estimation and propose a Compressed - Sensing based channel estimation with pilots super-imposed on data symbols.

TABLE OF CONTENTS

LIST OF FIGURES

CHAPTER 1

INTRODUCTION

The emergence of next-generation wireless networks, including 5G networks, is expected to bring forth a range of new use cases and business models driven by evolving user and system operator requirements. These networks need to address mobility demands, which are defined by the relative speed between users and the network edge, while ensuring a consistent user experience. For instance, in-vehicle mobile broadband service requires support for mobility speeds of up to 500 km/h for bullet trains and 1000 km/h for airplanes. In such high-mobility scenarios, wireless channels exhibit double selectivity, leading to inter-symbol interference caused by multipath effects (frequency selectivity) and Doppler shifts (time selectivity).

Orthogonal frequency division multiplexing (OFDM) is a wideband signaling technique that achieves orthogonality in the frequency domain by allocating information symbols to appropriately spaced subcarriers, thus enabling multiple symbols to overlap in time. This technique allows for multiple access by allocating orthogonal time-frequency resources to users. Even in the presence of multipath channel impairments, OFDM maintains orthogonality at the receiver, offering advantages such as low processing costs for detection and channel estimation.

However, there are some challenges to attain this goal. Particularly the presence of high Doppler shift caused by high-speed movement of terminals in the system, which leads to frequency spreading. This frequency spreading, in turn, introduces inter-carrier interference (ICI) in orthogonal frequency division multiplexing (OFDM) systems. Consequently, the performance of channel estimation and data detection is compromised, making it difficult to meet the requirements of highly reliable communication.

Recently, a novel modulation technique known as orthogonal time frequency space (OTFS) has been proposed, offering notable advantages over OFDM in delay-Doppler

channels. By utilizing the delay-Doppler domain, which presents an alternative representation of the varying geometry of a channel involving mobile terminals and reflectors, OTFS introduces a new approach.

In OTFS, the modulator spreads each information symbol across a two-dimensional orthogonal basis function, spanning the entire time-frequency domain required for transmitting a frame. This design takes advantage of full diversity over time and frequency. When combined with equalization, OTFS transforms the fading, time-varying wireless channel encountered by modulated signals like OFDM into a time-independent channel characterized by a roughly constant complex channel gain for all symbols.

In wireless systems, Channel Estimation holds significant importance as the accuracy of the estimation directly impacts data detection performance. The delay-Doppler (DD) representation of the wireless channel exhibits sparsity, allowing it to be effectively modeled using only a few taps. Each tap within the DD representation is defined by three key parameters: the tap's coefficient, delay, and Doppler characteristics.We study the Channel Estimation techniques proposed so far in the literature and also look at our new technique based on Compressed Sensing and compare it with the rest based on metrics like pilot overhead and BER performance.

Throughout the material, we utilize the following notation. We denote scalar, vector, and matrix variables as a, $\mathbf{a}$, and $\mathbf{A}$, respectively. The expressions $a(n)$ and $\mathbf{A}(m,n)$ refer to the nth element of vector $\mathbf{a}$ and the element at position (m,n) in matrix $\mathbf{A}$, respectively. The notations $\mathbf{A}^{\mathrm{H}}$ and $\mathbf{A}^n$ represent the Hermitian transpose and the nth power of matrix $\mathbf{A}$, respectively. The symbol $\mathbb{C}^{M\times N}$ represents the set of matrices with dimensions $M\times N$, where each element is drawn from the complex plane. The operator $\otimes$ denotes the Kronecker product. We define $\mathbf{A} = \operatorname{diag}\left[\mathbf{A}_0,\ldots,\mathbf{A}_{N-1}\right] \in \mathbb{C}^{MN\times MN}$ as a block diagonal matrix, composed of diagonal blocks $\mathbf{A}_0,\mathbf{A}_1,\ldots,\mathbf{A}_{N-1}$, each belonging to $\mathbb{C}^{M\times M}$. Additionally, we introduce $\mathbf{F}_n = \{\frac{1}{\sqrt{n}}e^{2\pi jkl/n}\}_{k,l=0}^{n-1}$ and $\mathbf{F}_n^{\mathrm{H}}$ as the n-point Discrete Fourier Transform (DFT) and Inverse Discrete Fourier Transform (IDFT) matrices, respectively. The term $\mathbf{I}_M$ represents an M-dimensional identity matrix.

CHAPTER 2

WIRELESS CHANNEL MODEL

The impulse response of a linear time-varying multipath channel can be modeled using various representations, depending on the chosen parameters (independent variables). These parameters include time (t), frequency (f), delay (τ), and Doppler (ν). The impulse response can be expressed in terms of time-frequency ($H(t, f)$), time-delay ($h(t, \tau)$), and delay-Doppler ($h(\tau, \nu)$) functions.

2.1 Delay-Doppler Representation

The channel's response to an impulse with delay τ and Doppler ν is described by the complex baseband channel impulse response, denoted as $h(\tau, \nu)$. When an input signal $s(t)$ is transmitted through this channel, the received signal can be expressed as:

$$r(t) = \iint h(\tau, \nu) s(t - \tau) e^{j2\pi\nu(t-\tau)} \mathrm{d}\nu \mathrm{d}\tau$$

One notable advantage of the $h(\tau, \nu)$ representation is its compactness. Typically, the number of channel reflectors with associated Dopplers is small, which means that fewer parameters are required for channel estimation in the delay-Doppler domain compared to the time-frequency domain. This sparse representation of typical channel models, including those in LTE, has significant implications for tasks such as channel estimation, equalization, and tracking.

2.2 Relation among different Channel Models

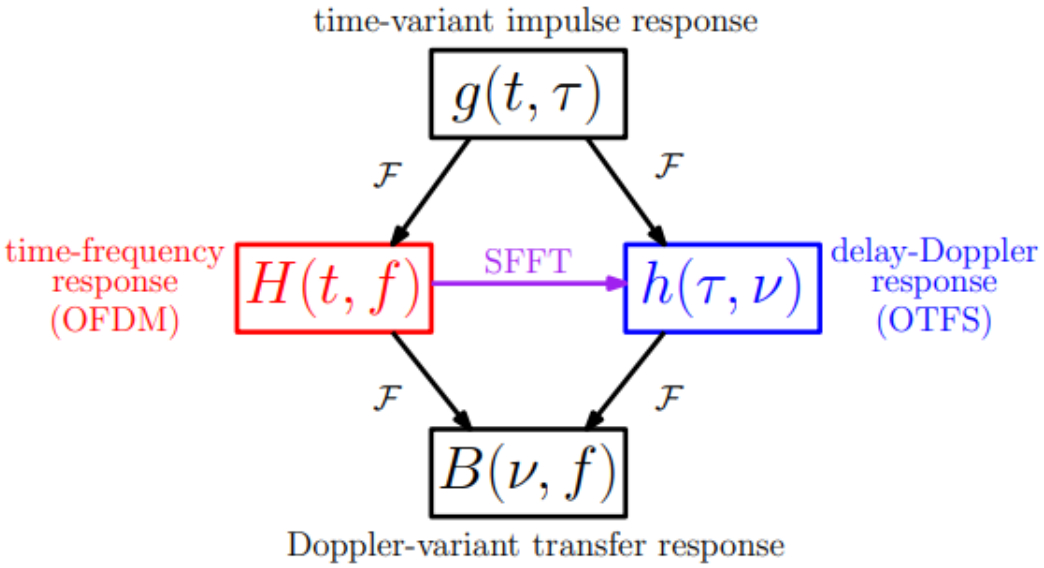

Figure 2.1: Relation between different wireless channel representation

- The received signal in linear time variant channel (LTV) can be represented as

$$
\begin{aligned}
r(t) &= \int \underbrace{g(t,\tau)}_{\text{time-variant impulse response}} s(t-\tau)d\tau \rightarrow \text{generalization of LTI} \\
&= \iint \underbrace{h(\tau,\nu)}_{\text{Delay-Doppler spreading function}} s(t-\tau)e^{j2\pi\nu t}d\tau d\nu \rightarrow \text{ Delay-Doppler Channel} \\
&= \int \underbrace{H(t,f)}_{\text{time-frequency response}} S(f)e^{j2\pi ft}df \rightarrow \text{ Time-Frequency Channel}
\end{aligned}
$$

- Relation between $h(\tau,\nu)$ and $H(t,f)$

$$
\left.
\begin{aligned}
h(\tau,\nu) &= \iint H(t,f)e^{-j2\pi(\nu t - f\tau)}dtdf \\
H(t,f) &= \iint h(\tau,\nu)e^{j2\pi(\nu t - f\tau)}d\tau d\nu
\end{aligned}
\right\} \text{ Pair of 2D symplectic FT}
$$

2.3 Sparsity & Slow Variability of Channel in Delay-Doppler Domain

In the time-frequency representation ($H(t, f)$) and time-delay representation ($h(t, \tau)$) of the channel, the channel coefficients exhibit variations over time at a rate inversely proportional to coherence time. This rate of variation depends on the mobility and operating frequency, leading to rapid changes in the channel state and making channel estimation challenging.

A more concise and equivalent representation of the channel is achieved in the delay-Doppler domain impulse response, $h(\tau, \nu)$. In this representation, the channel coefficients (taps) correspond to groups of reflectors with specific delay values determined by the relative distance of the reflectors, and Doppler values determined by the relative velocity between the transmitter and receiver. The velocity and distance tend to remain relatively constant for a few milliseconds. As a result, the channel in the delay-Doppler domain appears time-invariant over a longer observation duration compared to the time-frequency representation.

Furthermore, the delay-Doppler representation of the channel impulse response leads to a sparse representation of the time-varying channel. This sparsity allows for the estimation of fewer channel parameters, reducing the complexity of channel estimation.

Figure 2.1 depicts an example scenario encountered in urban multi-lanes. The figure illustrates a transmitter mounted atop a bus bay transmitting a signal intended for a moving car (depicted in blue). The transmitted signal undergoes reflection from multiple mobile reflectors (other cars) before reaching the receiver. To aid comprehension, we consider four paths corresponding to four reflectors, each indicated by a different color.

The impulse response of the wireless channel in this scenario is illustrated in both the delay-Doppler and time-frequency domains within the same figure, at time $t = t_0$ and $t = t_0 + \Delta$. Observing the figure, it becomes evident that the channel representation in the delay-Doppler domain exhibits sparsity compared to the time-frequency representation. Moreover, as the channel coefficients in the delay-Doppler representation cor-

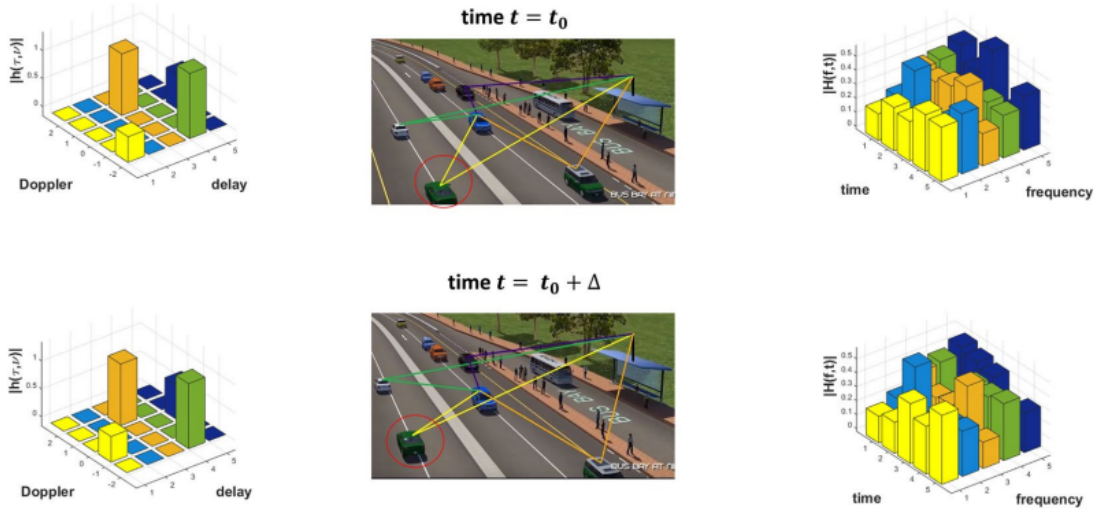

Figure 2.2: Example of a wireless channel in an urban multi-lane scenario illustrating the sparsity and slow variability of the channel in the delay–Doppler representation

respond to groups of reflectors with specific delay and Doppler shift, we observe four non-zero channel coefficients corresponding to the four reflectors in the figure. This emphasizes the sparse nature of the delay-Doppler representation, effectively capturing the wireless environment's geometry.

Figure 2.1 also showcases the channel at $t = t_0 + \Delta$, where one of the reflectors (circled in green) decelerates. Consequently, the coefficient associated with this reflector now resides in a different bin on the Doppler axis (indicated by the yellow bar) within the delay-Doppler grid. Conversely, the coefficients corresponding to other reflectors remain in their respective bins at time t_0. However, the time-frequency representation of the channel exhibits significant variation at times t_0 and $t_0 + \Delta$. This highlights the slower variability of the channel in the delay-Doppler representation compared to the time-frequency representation.

CHAPTER 3

REVIEW ON OFDM

Orthogonal Frequency Division Multiplexing (OFDM) serves as a fundamental modulation scheme extensively utilized in 4G/5G mobile communication systems. This wideband multicarrier scheme involves the multiplexing of information symbols onto closely spaced orthogonal subcarriers. By maintaining the orthogonality of these subcarriers, data can be transmitted simultaneously on multiple channels. The key advantage lies in the orthogonality property, which enables the use of a single tap equalizer for reliable detection of transmitted data at the receiver. As a result, this approach offers a low-complexity solution for achieving dependable communication in frequency selective channels, such as the static multipath wireless channel.

While OFDM with cyclic prefix (CP) has been the predominant waveform choice for 4G/5G systems, it encounters certain drawbacks. These include a high peak-to-average power ratio (PAPR), susceptibility to carrier frequency offsets (CFO), and significant loss of orthogonality in high-mobility wireless channels.

3.1 OFDM System Model

OFDM is designed to efficiently transmit data over a wide frequency band by dividing it into multiple narrow subcarriers. These subcarriers are closely spaced in the frequency domain and are orthogonal to each other, meaning they do not interfere with one another.

Here's a step-by-step explanation of how OFDM works:

- **Subcarrier Generation**: The original wideband signal is divided into a large number of narrow subcarriers. The subcarriers are typically orthogonal to each other, meaning they have no overlapping frequency content.
- **Modulation**: Each subcarrier is independently modulated using a digital modulation scheme such as Quadrature Amplitude Modulation (QAM) or Phase Shift Keying (PSK). The choice of modulation scheme depends on the system requirements and channel conditions.

- **IFFT and CP Insertion**: In the frequency domain, the modulated subcarriers are combined using an Inverse Fast Fourier Transform (IFFT), which converts them into the time domain. Additionally, a cyclic prefix (CP) is inserted at the beginning of each OFDM symbol. The cyclic prefix is a copy of the latter part of the symbol and helps to combat inter-symbol interference caused by multipath propagation.
- **Serial-to-Parallel Conversion**: The resulting time-domain OFDM symbol is converted from a serial stream into parallel data streams, with each stream representing the modulated data on each subcarrier.
- **Transmission**: The parallel streams are sent over the wireless channel concurrently, exploiting the frequency diversity provided by the closely spaced subcarriers. OFDM's robustness to frequency-selective fading and multipath propagation allows reliable communication in challenging environments.
- **Reception**: At the receiver, the received signal is demodulated by performing the reverse process. The cyclic prefix is removed, and the time-domain signal is transformed back into the frequency domain using a Fast Fourier Transform (FFT). Each subcarrier is then demodulated, and the original data is recovered.

By dividing the available spectrum into multiple orthogonal subcarriers, OFDM provides high spectral efficiency and robustness against frequency-selective fading and interference. It is a key technology that enables high-speed data transmission and efficient spectrum utilization in modern wireless communication systems.

Figure 3.1 and 3.2 summarises the transmitter and receiver operation of OFDM.

We will now look into the input-output relation in ODFM. We assume the channel to be constant over 1 OFDM symbol and no Doppler present in the channel. Let $h_0, h_1, \cdots, h_{P-1}$ be the path gains over P multipath. The received signal r can be expressed as

$$\mathbf{r} = \underbrace{\begin{bmatrix} h_0 & 0 & \cdots & 0 & h_{P-1} & h_{P-2} & \cdots & h_1 \\ h_1 & h_0 & \cdots & 0 & 0 & h_{P-1} & \cdots & h_2 \\ \vdots & \ddots & \ddots & \ddots & \ddots & \ddots & \ddots & \vdots \\ 0 & 0 & \cdots & h_{P-1} & h_{P-2} & \cdots & h_1 & h_0 \end{bmatrix}}_{\text{Circulant matrix } (\mathbf{H})} \mathbf{s} + \mathbf{w}$$

$$= \sum_{i=0}^{P-1} h_i \mathbf{\Pi}^i \mathbf{s}; \mathbf{\Pi} \text{ is the permutation matrix, } \begin{bmatrix} 0 & 0 & 1 & \\ 1 & \ddots & 0 & 0 \\ \vdots & \ddots & \ddots & \vdots \\ 0 & \cdots & 1 & 0 \end{bmatrix} \text{ (notation used later)}$$

$$= \mathbf{F}^H \mathbf{D} \mathbf{F} \mathbf{s}$$

Note, $\mathbf{y} = \mathbf{F}\mathbf{r}$ and $s = \mathbf{F}^H \mathbf{x}$, hence

$$\mathbf{y} = \underbrace{\mathrm{D}}_{\text{Diagonal matrix}} \mathbf{x}$$

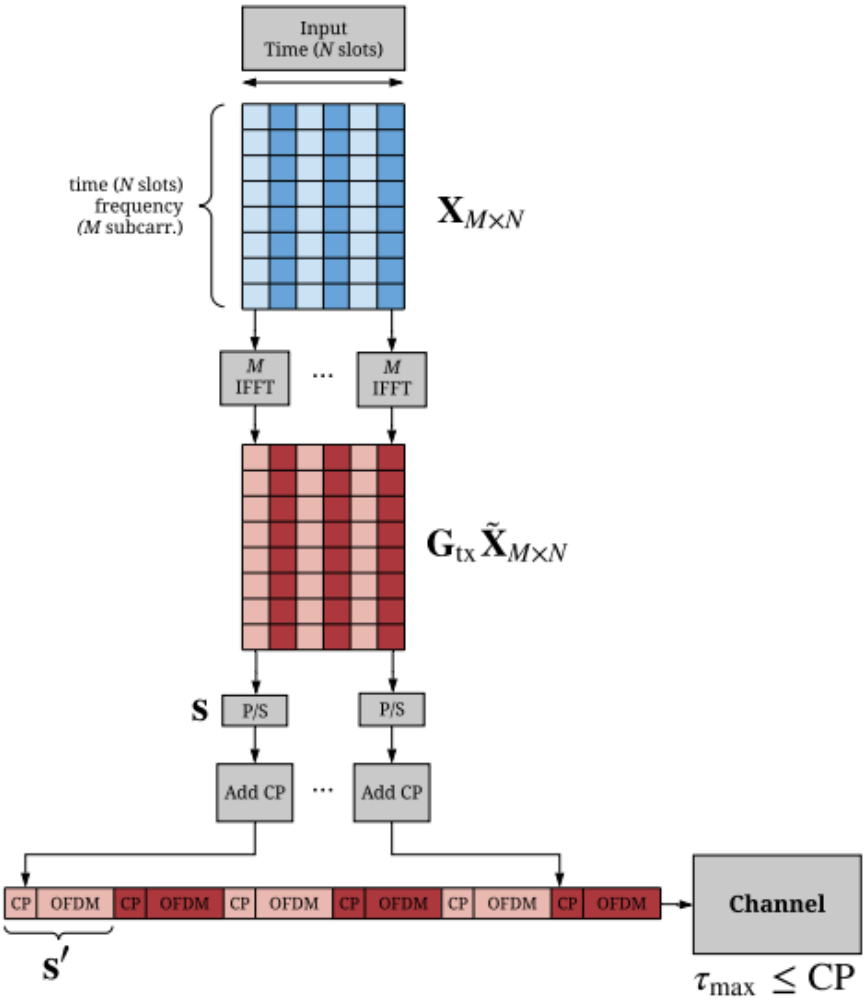

Figure 3.1: OTFS Transmitter

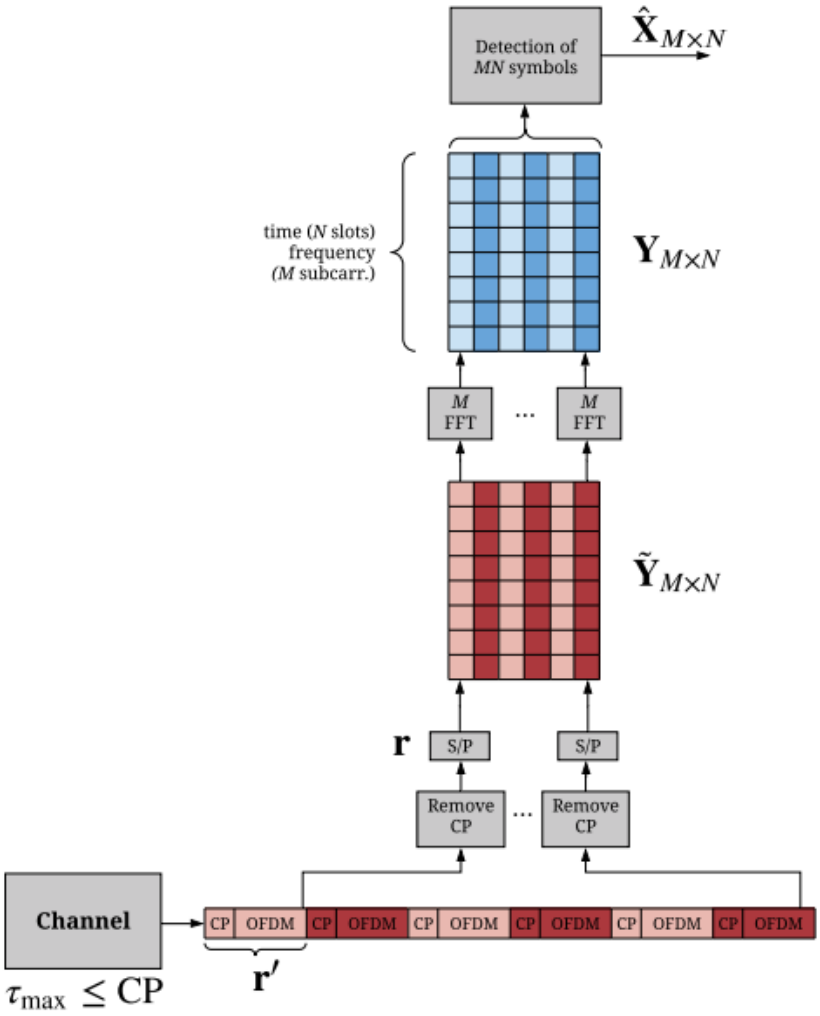

Figure 3.2: OFDM Receiver

To summarize, OFDM (Orthogonal Frequency Division Multiplexing) exhibits the following key characteristics:

- OFDM employs multiple subcarriers to transmit information, ensuring that all subcarriers are orthogonal to each other under specific conditions.
- Each OFDM symbol is prefixed with a cyclic prefix (CP) of length lmax, which serves to counteract the effects of severe multipath channel delay spread and inter-symbol interference (ISI).
- The CP introduces a circulant channel matrix structure, which facilitates single-tap equalization to mitigate the impact of severe multipath channel impairments.

Overall, OFDM offers a modulation and demodulation scheme with low complexity, leveraging the Fast Fourier Transform (FFT) and the CP.

3.2 Limitations of OFDM

Let us now look into few of the limitations faced by OFDM modulation technique.

3.2.1 High PAPR

The PAPR is the ratio between the maximum power of a time domain sample in an OFDM transmit symbol and the average power of OFDM symbol, defined as

$$\mathrm{PAPR_{dB}} \triangleq 10\log_{10}\frac{\max\left\{|\mathbf{s}[m]|^2\right\}}{\mathrm{E}\left\{|\mathbf{s}[m]|^2\right\}}, m = 0, \ldots, M-1,$$

where

$$\mathrm{s}[m] = \frac{1}{\sqrt{M}}\sum_{k=0}^{M-1}\mathrm{x}[k]e^{\frac{[2\pi km}{M}}.$$

Note that $\mathrm{E}\left(|\mathbf{x}[k]|^2\right) = E_s, \mathrm{E}(\mathrm{x}[k]) = 0$, for all k, and

$$\begin{aligned}
\mathrm{E}\left(|\mathbf{s}[m]|^2\right) &= \mathrm{E}\left(\frac{1}{M}\sum_{k=0}^{M-1}\sum_{k'=0}^{M-1}\mathbf{x}[k]\mathbf{x}^*\left[k'\right]e^{\frac{|2\mathrm{r}(k-k')\mathrm{m}}{M}}\right) \\
&= \frac{1}{M}\sum_{k=0}^{M-1}\sum_{k'=0}^{M-1}\mathrm{E}\left(\mathbf{x}[k]\mathbf{x}^*\left[k'\right]\right)e^{\frac{[2\pi(k-k')\mathrm{m}}{M}} \\
&= \frac{1}{M}(\sum_{k=0}^{M-1}\underbrace{\mathrm{E}\left(|\mathbf{x}[k]|^2\right)}_{=E_S} + \sum_{k=0}^{M-1}\sum_{k'=0,k'\neq k}^{M-1}\underbrace{\mathrm{E}(\mathbf{x}[k])\mathrm{E}\left(\mathbf{x}^*\left[k'\right]\right)}_{=0}e^{\frac{[2\pi(k-k'\,\mathrm{mom}}{M}}) \\
&= E_s.
\end{aligned}$$

Assuming $|\mathbf{x}[k]|^2 = A^2$, for all k, where A^2 denotes the peak power constellation point with

$$A^2 = \alpha E_s \text{ and } \alpha \geq 1,$$

we obtain

$$\max\left(|\mathbf{s}[m]|^2\right) = |\mathbf{s}[0]|^2 = \left|\frac{1}{\sqrt{M}}\sum_{k=0}^{M-1}\mathbf{x}[k]\right|^2 = MA^2.$$

Hence, PAPR in OFDM is

$$\mathrm{PAPR_{dB}} = \frac{MA^2}{E_S} = \alpha M.$$

It is important to note that when the value of α is greater than or equal to 1 (typically observed when M is a large number), the Peak-to-Average Power Ratio (PAPR) can become significantly high. This phenomenon is primarily attributed to the Inverse Fast Fourier Transform (IFFT) operation, where the summation of data symbols across subcarriers can result in peak values in the signal. The presence of high peaks can force the power amplifier to operate in the nonlinear region, causing a degradation in system performance. Hence, reducing PAPR in OFDM systems is a critical issue that needs to be addressed.

3.2.2 Sensitivity to CFO

Frequency offset is a critical factor affecting Orthogonal Frequency Division Multiplexing (OFDM) systems. It can arise from discrepancies in transmitter and receiver frequencies or due to Doppler shifts resulting from the motion of either the transmitter or the receiver. When frequency offset occurs ($f_o = f_c - f_c^{'}$, here f_c and $f_c^{'}$ are the carrier frequencies in the transmitter and the receiver), the received signal becomes frequency-shifted, causing misalignment between the sampling points in the frequency domain and the center frequencies of the subcarriers.

As a consequence, the amplitudes of the intended subcarriers diminish, leading to a decrease in their desired signal strength. Additionally, intercarrier interference (ICI) emerges, further degrading the system's performance. A receiver will need to estimate the CFO $f_o = f_c - f_c^{'}$ using a pilot tone and then compensate for it by multiplying the output of the mixer by $\exp(-j2\pi\hat{f}_o t)$.

3.2.3 OFDM in high-mobility multi-path channel

In this section, we consider OFDM in a high-mobility multipath channel, where each path has different Doppler shifts $v_i = k_i/T$ for $i = 1, \ldots, P$. The time domain received signal is given by

$$\mathbf{r} = \mathbf{H}\mathbf{s} + \mathbf{w}$$

where $\mathbf{H}$ is a $M \times M$ matrix

$$\mathbf{H} = \sum_{i=1}^{P} h_i \mathbf{\Pi}^{l_i} \mathbf{\Delta}^{k_i}$$

The matrices $\mathbf{\Pi}^{l_i}$ and $\mathbf{\Delta}^{k_i}$ are utilized to represent the delays, and Doppler shifts within the l_i-th delay path. When the channel matrix $\mathbf{H}$ is multiplied by the signal vector $\mathbf{s}$, it implies that the l_i-th path introduces a cyclic shift of $\mathbf{s}$ by l_i steps, as characterized by $\mathbf{\Pi}^{l_i}$. Additionally, it modulates the shifted signal with a carrier at frequency k_i, modeled by $\mathbf{\Delta}^{k_i}$.

However, the presence of multiple Dopplers introduces additional complexity to $\mathbf{H}$, resulting in it no longer being a circulant matrix. Consequently, the eigenvalue decomposition of $\mathbf{H}$ cannot be relied upon, and severe intercarrier interference (ICI) emerges.

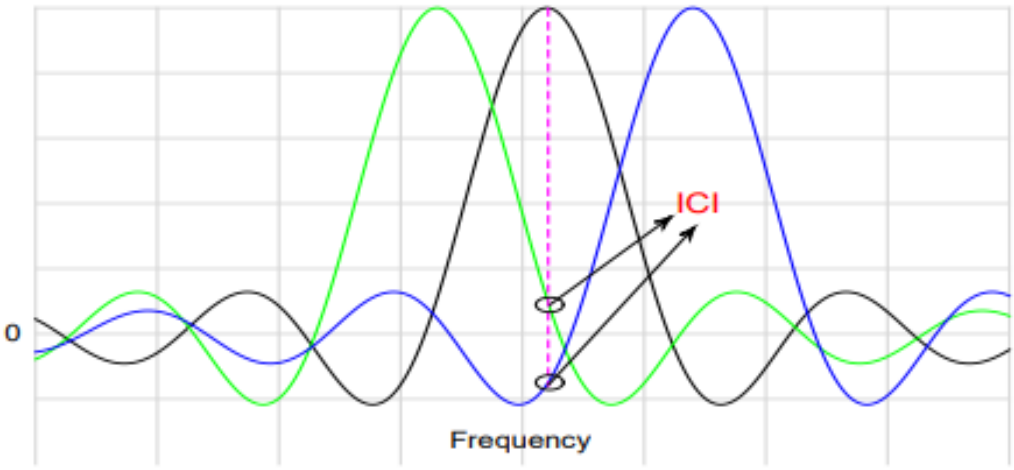

Figure 3.3: Inter Carrier Interference in OFDM - High Doppler scenario

To summarize, the presence of multiple Dopplers poses challenges for OFDM. It becomes difficult to equalize multiple Dopplers, and the subchannel gains are unequal, with the performance being dictated by the subchannel with the lowest gain. Therefore, the development of new modulation techniques is necessary to address the effects of high Doppler shifts effectively.

CHAPTER 4

DELAY-DOPPLER DOMAIN MODULATION

This section begins by reviewing the fundamental concepts in Orthogonal Time Frequency Space (OTFS) and subsequently presents a detailed analysis of the OTFS modulation and demodulation process. A key focus of this section is to derive the input-output relationship of OTFS modulation/demodulation specifically for delay-Doppler channels.

4.1 System Model

To discretize the time-frequency signal plane, we sample the time axis at intervals of T seconds and the frequency axis at intervals of Δf (Hz). This results in a grid representation of the plane denoted as $\Lambda = \{(nT, m\Delta f), n = 0, \ldots, N-1, m = 0, \ldots, M-1\}$, where N and M are positive integers.

Within the framework of OTFS, the modulated time-frequency samples $X_{tf}[n, m]$ are transmitted over an OTFS frame of duration $T_f = NT$ and occupy a bandwidth of $B = M\Delta f$. The transmit and receive pulses (or waveforms) are referred to as $g_{\text{tx}}(t)$ and $g_{\text{rx}}(t)$, respectively. We denote the cross-ambiguity function between $g_{\text{tx}}(t)$ and $g_{\text{rx}}(t)$ as $A_{g_{\text{rx}},g_{\text{tx}}}(t, f)$, defined as:

$$A_{g_{\text{rx}},g_{\text{tx}}}(t, f) \triangleq \int g^*_{\text{rx}}(t' - t)\, g_{\text{tx}}(t')\, e^{-j2\pi f(t'-t)} dt'$$

In the delay-Doppler plane, we discretize the plane into an information grid denoted as $\Gamma = \left\{ \left(\frac{k}{NT}, \frac{l}{M\Delta f} \right), k = 0, \ldots, N-1, l = 0, \ldots, M-1 \right\}$. Here, $1/M\Delta f$ and $1/NT$ represent the quantization steps of the delay and Doppler frequency, respectively.

Remark : (Choice of Parameters in OTFS Systems) In an OTFS communications system with given constraints on total bandwidth $B = M\Delta f$ and latency $T_f = NT$, it

is possible to choose appropriate values for N, M, and T (since $\Delta f = 1/T$) to enable communication over a time-varying channel with maximum delay $\tau_{\max}$ and maximum Doppler $\nu_{\max}$, considering all channel paths.

The parameters T and Δf play a crucial role in determining the maximum supported Doppler (i.e., $1/T$) and delay (i.e., $1/\Delta f$). Therefore, it is necessary to ensure that $\nu_{\max} < 1/T$ and $\tau_{\max} < 1/\Delta f$ in order to determine the values of N and M.

To maintain a fixed data rate of NM symbols per frame, different choices of T and Δf can be made based on the channel conditions. For instance, selecting a larger value of T and a smaller value of Δf would result in a smaller N and a larger M, respectively. Conversely, choosing a smaller T and a larger Δf would yield a larger N and a smaller M. The specific choice depends on the prevailing channel characteristics and desired system performance.

Figure 4.1 illustrates the block diagram of the OTFS system. OTFS modulation involves a series of transformations at both the transmitter and receiver. To achieve modulation, the modulator utilizes a pair of 2D transforms. Initially, the modulator maps the information symbols $\mathbf{X}[k,l]$ in the delay-Doppler domain to samples $\mathbf{X}_{tf}[n,m]$ in the time-frequency domain using the inverse symplectic finite Fourier transform (ISFFT). Subsequently, the Heisenberg transform is applied to $\mathbf{X}_{tf}[n,m]$ to generate the time-domain signal $\mathbf{s}(t)$ for transmission over the wireless channel.

Upon reception, the time-domain signal $\mathbf{r}(t)$ is first transformed to the time-frequency domain using the Wigner transform (the inverse of the Heisenberg transform). Then, the signal is further converted to the delay-Doppler domain using SFFT to facilitate symbol demodulation.

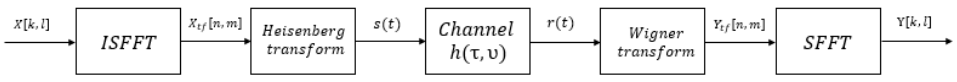

Figure 4.1: OTFS mod/demod

4.2 OTFS Modulation

Consider a set of NM information symbols $\{\mathbf{X}[k,l], k = 0,\ldots,N-1, l = 0,\ldots,M-1\}$ from a modulation alphabet of size Q $\mathbb{A} = \{a_1, \cdots, a_Q\}$ (e.g. QAM symbols), which are arranged on the delay-Doppler grid Γ.

The OTFS transmitter first maps symbols $\mathbf{X}[k,l]$ to NM samples $\mathbf{X}_{tf}[n,m]$ on the time-frequency grid Λ using the ISFFT as follows

$$\mathbf{X}[n,m] = \frac{1}{\sqrt{NM}} \sum_{k=0}^{N-1} \sum_{l=0}^{M-1} \mathbf{X}_{tf}[k,l] e^{j2\pi\left(\frac{nk}{N} - \frac{ml}{M}\right)}$$

for $n = 0,\ldots,N-1, m = 0,\ldots,M-1$.

Next, a time-frequency modulator converts the samples $X[n,m]$ to a continuous time waveform $\mathbf{s}(t)$ using a transmit waveform $g_{\text{tx}}(t)$ (discrete Heisenberg transform) as

$$\mathbf{s}(t) = \sum_{n=0}^{N-1} \sum_{m=0}^{M-1} \mathbf{X}_{tf}[n,m] g_{\text{tx}}(t-nT) e^{j2\pi m\Delta f(t-nT)}$$

We will now look at the Transmitter (OTFS Modulation) operation in the matrix operation terms.

Consider the two-dimensional information symbols transmitted in the delay-Doppler plane, denoted as $\mathbf{X} \in \mathbb{C}^{M\times N}$. To convert these symbols into time-frequency signals, Inverse Symplectic Fast Fourier Transform (ISFFT) precoding is applied. This involves performing an M-point FFT on the columns of $\mathbf{X}$ and an N-point IFFT on the rows of $\mathbf{X}$. The resulting time domain signal is generated by the "Heisenberg transform modulator," which utilizes an M-point IFFT along with the pulse-shaping waveform $g_{\text{tx}}(t)$. We can express the transmitted signal $\mathbf{S}$ as:

$$\mathbf{S} = \mathbf{G}_{\text{tx}} \mathbf{F}_M^{\text{H}} \left(\mathbf{F}_M \mathbf{X} \mathbf{F}_N^{\text{H}}\right) = \mathbf{G}_{\text{tx}} \mathbf{X} \mathbf{F}_N^{\text{H}}$$

Here, the diagonal matrix $\mathbf{G}_{\text{tx}}$ contains the samples of $g_{\text{tx}}(t)$ as its entries, given by $\mathbf{G}_{\text{tx}} = \text{diag}\left[g_{\text{tx}}(0), g_{\text{tx}}(T/M), \ldots, g_{\text{tx}}((M-1)T/M)\right] \in \mathbb{C}^{M\times M}$. For rectangular

waveforms, $\mathbf{G}_{\text{tx}}$ reduces to the identity matrix $\mathbf{I}M$.

By column-wise vectorization of the $M \times N$ matrix $\mathbf{S}$ from equation (1), we obtain the $MN \times 1$ vector $\mathbf{s} = \text{vec}(\mathbf{S})$, which can be expressed as:

$$\mathbf{s} = \text{vec}(\mathbf{S}) = \left(\mathbf{F}_N^{\text{H}} \otimes \mathbf{G}_{\text{tx}}\right) \mathbf{x}$$

Here, $\mathbf{x} = \text{vec}(\mathbf{X})$, and $\otimes$ represents the Hadamard product. It is assumed that a cyclic prefix (CP) of length $L - 1$ is appended to $\mathbf{s}$ before transmission.

4.3 Wireless Transmission

After undergoing parallel-to-serial and digital-to-analog conversion, with the transmitted signal denoted as $\mathbf{s}(t)$, the received signal $\mathbf{r}(t)$ can be represented as

$$r(t) = \iint h(\tau, \nu) s(t - \tau) e^{j2\pi\nu(t-\tau)} d\tau d\nu + w(t)$$

Considering that the channel typically contains a limited number of reflectors with associated delays and Doppler shifts, it often requires only a few parameters to characterize the channel in the delay-Doppler domain. Given the sparse nature of the channel representation, it is convenient to express the response $h(\tau, \nu)$ using the following form:

$$h(\tau, \nu) = \sum_{i=1}^{P} h_i \delta\left(\tau - \tau_i\right) \delta\left(\nu - \nu_i\right)$$

In the above equation, $\delta(\cdot)$ represents the Dirac delta function, P denotes the number of propagation paths, and h_i, τ_i, and ν_i correspond to the complex path gain, delay, and Doppler shift (or frequency) associated with the i-th path, respectively. The delay and Doppler-shift taps for the i-th path can be expressed as follows:

$$\tau_i = \frac{l_i}{M\Delta f}, \quad \nu_i = \frac{k_i}{NT}$$

To facilitate the derivations, we make the assumption that the delay and Doppler shifts are integer multiples of $\frac{1}{M\Delta f}$ and $\frac{1}{NT}$ respectively. In other words, we assume

that l_i and k_i are integers.

In LTE channels, typical values of l_i and k_i are less than 10% of M and N respectively. The received signal $y(t)$ is sampled at a rate $f_s = M\Delta f = \frac{M}{T}$, and after discarding the cyclic prefix (CP), a vector $\mathbf{r} = \{r(n)\}_{n=0}^{MN-1}$ is formed.

$$r(n) = \sum_{i=1}^{P} h_i e^{j2\pi \frac{k_i(n-l_i)}{MN}} s\left([n-l_i]_{MN}\right) + w(n)$$

where $[\cdot]_n$ denotes mod- n operation. We write the above equation in vector form as

$$\mathbf{r} = \mathbf{H}\mathbf{s} + \mathbf{w}$$

where $\mathbf{H}$ is the $MN \times MN$ matrix

$$\mathbf{H} = \sum_{i=1}^{P} h_i \mathbf{\Pi}^{l_i} \mathbf{\Delta}^{k_i}$$

with Π the permutation matrix (forward cyclic shift),

$$\mathbf{\Pi} = \begin{bmatrix} 0 & \cdots & 0 & 1 \\ 1 & \ddots & 0 & 0 \\ \vdots & \ddots & \ddots & \vdots \\ 0 & \cdots & 1 & 0 \end{bmatrix}_{MN \times MN}$$

and $\mathbf{\Delta}$ is the $MN \times MN$ diagonal matrix

$$\mathbf{\Delta} = \operatorname{diag}\left[z^0, z^1, \ldots, z^{MN-1}\right]$$

with $z = e^{\frac{j2\pi}{MN}}$. Here, the matrices $\mathbf{\Pi}$ and $\mathbf{\Delta}$ model the delays and the Doppler shifts, respectively. Each path introduces an l_i-step cyclic shift of the transmitted signal vector $\mathbf{s}$, modeled by Π^{l_i}, and modulates it with a carrier at frequency k_i, modeled by Δ^{k_i}.

4.4 OTFS Demodulation

At the receiver, a matched filter computes the crossambiguity function $A_{g_{\mathrm{rx}},r}(t,f)$ as follows

$$Y(t,f) = A_{g_{\mathrm{rx}},r}(t,f) \triangleq \int g_{\mathrm{rx}}^{*}\left(t'-t\right) r\left(t'\right) e^{-j2\pi f(t'-t)} dt'$$

The matched filter output is obtained by sampling $Y(t,f)$ as

$$\mathbf{Y}_{tf}[n,m] = Y(t,f)|_{t=nT, f=m\Delta f}$$

Next, the SFFT is applied on the samples $\mathbf{Y}_{tf}[n,m]$ to obtain symbols $\mathbf{Y}[k,l]$ in the delay-Doppler domain

$$\mathbf{Y}[k,l] = \frac{1}{\sqrt{NM}} \sum_{n=0}^{N-1} \sum_{m=0}^{M-1} \mathbf{Y}_{tf}[n,m] e^{-j2\pi\left(\frac{nk}{N} - \frac{ml}{M}\right)}.$$

We will now look at the Receiver (OTFS Demodulation) operation in the matrix operation terms.

At the receiver, we perform operations that reverse those of the transmitter in order to convert the received signal samples $\mathbf{r}$ into time-frequency domain symbols $\mathbf{R}$ (where the vector elements are reshaped into a matrix) and then into delay-Doppler domain symbols $\mathbf{Y}$ using the following transformations: $\mathbf{Y} = \mathbf{F}_M^{\mathrm{H}} \left(\mathbf{F}_M \mathbf{G}_{\mathrm{rx}} \mathbf{R}\right) \mathbf{F}_N$. This involves applying an M-point FFT followed by an SFFT. Here, $\mathbf{G}\mathrm{rx} \in \mathbb{C}^{M \times M}$ represents the filter employed at the receiver, which corresponds to the pulse-shaping waveform $g_{\mathrm{rx}}(t)$. Here, the diagonal matrix $\mathbf{G}_{\mathrm{rx}}$ contains the samples of $g_{\mathrm{rx}}(t)$ as its entries, and it can be expressed as $\mathbf{G}_{\mathrm{rx}} = \mathrm{diag}\left[g_{\mathrm{rx}}(0), g_{\mathrm{rx}}(T/M), \ldots, g_{\mathrm{rx}}((M-1)T/M)\right]$.

In vectorized form the received signal in the delay-Doppler domain can be written as

$$\begin{aligned}
\mathbf{y} &= \left(\mathbf{F}_N \otimes \mathbf{G}_{\mathrm{rx}}\right) \mathbf{r} \\
&= \left(\mathbf{F}_N \otimes \mathbf{G}_{\mathrm{rx}}\right) \mathbf{H} \left(\mathbf{F}_N^{\mathrm{H}} \otimes \mathbf{G}_{\mathrm{tx}}\right) \mathbf{x} + \left(\mathbf{F}_N \otimes \mathbf{G}_{\mathrm{rx}}\right) \mathbf{w} \\
&= \mathbf{H}_{\mathrm{eff}} \mathbf{x} + \widetilde{\mathbf{w}}
\end{aligned}$$

where $\mathbf{H}_{\mathrm{eff}} = \left(\mathbf{F}_N \otimes \mathbf{G}_{\mathrm{rx}}\right) \mathbf{H} \left(\mathbf{F}_N^{\mathrm{H}} \otimes \mathbf{G}_{\mathrm{tx}}\right)$ denotes the effective channel matrix, and $\widetilde{\mathbf{w}} = \left(\mathbf{F}_N \otimes \mathbf{G}_{\mathrm{rx}}\right) \mathbf{w}$ the noise vector. It can be easily seen that in general $\widetilde{\mathbf{w}}$ has a di-

agonal covariance matrix, which becomes a scalar matrix (indicating iid noise samples) in the case of rectangular waveforms, i.e., $\mathbf{G}_{\mathrm{rx}} = \mathbf{I}_M$.

4.5 Input-Output Relation - Vectorized Form

In this section, we begin by deriving the simplified form of $\mathbf{H}_{\text{eff}}$ specifically for rectangular waveforms. We then proceed to generalize this relation for arbitrary waveforms employed at both the transmitter and receiver. When using rectangular waveforms, both $\mathbf{G}_{\mathrm{tx}}$ and $\mathbf{G}_{\mathrm{rx}}$ are equal to the identity matrix $\mathbf{I}_M$, and as a result, we have the following relationship:

$$\mathbf{H}_{\text{eff}}^{\text{rect}} = \left(\mathbf{F}_N \otimes \mathbf{I}_M\right) \mathbf{H} \left(\mathbf{F}_N^{\mathrm{H}} \otimes \mathbf{I}_M\right)$$

Because $\mathbf{H} = \sum_{i=1}^{P} h_i \mathbf{\Pi}^{l_i} \mathbf{\Delta}^{k_i}$, we can further simplify $\mathbf{H}_{\text{eff}}^{\text{rect}}$ as

$$\mathbf{H}_{\text{eff}}^{\text{rect}} = \sum_{i=1}^{P} h_i \underbrace{\left[\left(\mathbf{F}_N \otimes \mathbf{I}_M\right) \mathbf{\Pi}^{l_i} \left(\mathbf{F}_N^{\mathrm{H}} \otimes \mathbf{I}_M\right)\right]}_{\mathbf{P}^{(i)}}$$
$$\cdot \underbrace{\left[\left(\mathbf{F}_N \otimes \mathbf{I}_M\right) \mathbf{\Delta}^{k_i} \left(\mathbf{F}_N^{\mathrm{H}} \otimes \mathbf{I}_M\right)\right]}_{\mathbf{Q}^{(i)}} = \sum_{i=1}^{P} h_i \mathbf{P}^{(i)} \mathbf{Q}^{(i)}$$

The received signal vector $\mathbf{y}$, by substituting $\mathbf{H}_{\text{eff}}^{\text{rect}}$, can be expressed as follows

$$\mathbf{y} = \left(\sum_{i=1}^{P} h_i \mathbf{\Gamma}_i\right) \mathbf{x} + \tilde{\mathbf{w}}.$$

The matrix $\mathbf{\Gamma}_i = \mathbf{P}^{(i)} \mathbf{Q}^{(i)} \in \mathbb{C}^{MN \times MN}$. The received vector can be succinctly written as

$$\mathbf{y} = \mathbf{\Omega} \mathbf{h} + \tilde{\mathbf{w}}.$$

The concatenated matrix $\mathbf{\Omega} \in \mathbb{C}^{MN \times P}$ data vector $\mathbf{x}_d$ is obtained as follows

$$\mathbf{\Omega} = \begin{bmatrix} \mathbf{\Gamma}_1 \mathbf{x} & \mathbf{\Gamma}_2 \mathbf{x} & \cdots & \mathbf{\Gamma}_P \mathbf{x} \end{bmatrix}$$

Therefore, the OTFS system (Input-Output Relation) can be expressed as follows depending on the problem in hand.

$$\mathbf{y} = \mathbf{\Omega h} + \tilde{\mathbf{w}}.$$

$$\mathbf{y} = \mathbf{H}_{\text{eff}}\mathbf{x} + \widetilde{\mathbf{w}}$$

where, $\mathbf{y}, \mathbf{x}, \widetilde{\mathbf{w}} \in \mathbb{C}^{MN\times 1}$, $\mathbf{h} \in \mathbb{C}^{P\times 1}$ and $\mathbf{\Omega} \in \mathbb{C}^{MN\times P}$, $\mathbf{H}_{\text{eff}} \in \mathbb{C}^{MN\times MN}$. It is also possible to model $\mathbf{h} \in \mathbb{C}^{MN\times 1}$ with only P non-zero entries in a $MN \times 1$ vector and $\mathbf{\Omega} \in \mathbb{C}^{MN\times MN}$.

We will now look into some simulation results to illustrate the performance of an OTFS system compared to an OFDM system. For this study, we consider an OTFS system with the number of delay bins $M = 16$, the Doppler bins $N = 32$, and set the carrier frequency and subcarrier spacing as 4 GHz and 15 KHz, respectively. The system uses a rectangular pulse and symbols are drawn from 4-QAM constellation. We assume a static multi-path channel with 6 delay taps, and the length of cyclic-prefix to be 6 as well. Figure 4.2 is the channel model that we will adopt for all the simulations in this study here afterwards.

$\boldsymbol{Path\ (i)}$	1	2	3	4	5
$\boldsymbol{Delay\ (\tau_i, \mu s)}$	4.2	8.4	12.6	16.8	21
$\boldsymbol{Doppler\ (\vartheta_i, Hz)}$	0	470	940	1410	1880

Figure 4.2: delay-Doppler channel model

From Figure 4.3 it is evident that OTFS is shown to exhibit significantly lower bit error rates than OFDM.The OTFS transform spreads each QAM symbol over all time and frequency dimensions of the channel and then extracts the resulting full diversity, while OFDM limits the transmission to a narrow subchannel of N subcarriers. OTFS operates in the delay-Doppler coordinate system and we show that with this modulation scheme coupled with equalization, all modulated symbols experience the same channel gain extracting the full channel diversity.

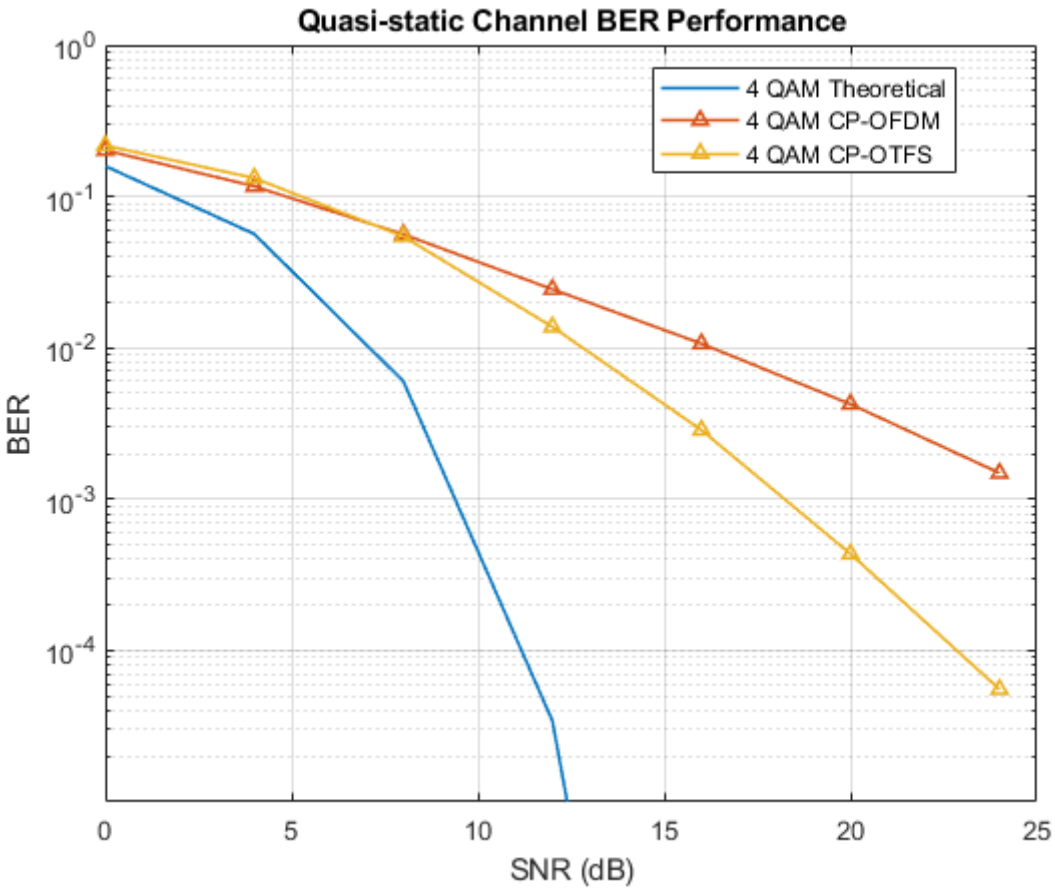

Figure 4.3: OFDM vs OTFS Performance Comparison

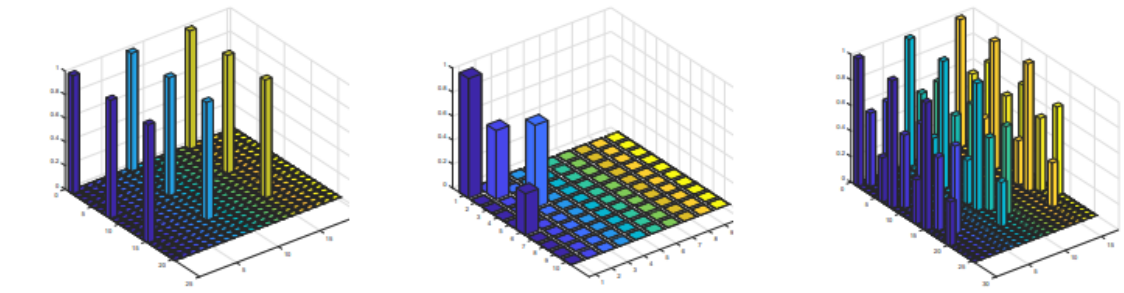

(a) Input signal, $x[k, l]$ (b) Channel, $h[k, l]$ (c) Output signal, $y[k, l]$

Figure 4.4: OTFS signals : 2D Circular Convolution with channel response

CHAPTER 5

STATE-OF-THE-ART CHANNEL ESTIMATION TECHNIQUES

OTFS (Orthogonal Time Frequency Space) is an innovative modulation technique that has demonstrated resilient performance in environments characterized by high mobility. Unlike traditional multicarrier modulation methods that operate in the time-frequency (TF) domain, OTFS modulation relies on the representation of the channel and the multiplexing of information symbols in the delay-Doppler (DD) domain.

In the context of OTFS, the delay-Doppler channel response serves as a parameterization of the impact of a time-varying channel on a transmitted waveform. This response, formulated in the delay-Doppler domain, effectively represents the influential scatterers within the channel, characterized by their individual delay and Doppler parameters. In the time-frequency domain, this can be equivalently understood as a conventional time-varying impulse response. This fundamental principle of OTFS modulation offers significant benefits.

One key advantage of the DD representation of wireless channels is that it renders rapidly time-varying channels nearly time-invariant when observed in the DD domain. This means that the channel in the DD domain appears stationary for an extended period, simplifying the task of channel estimation in channels with rapid time variations compared to estimation in the TF domain. Furthermore, the channel in the DD domain exhibits a sparse representation, necessitating the estimation of only a few parameters at the receiver.

Estimating delay-Doppler channel response at the receiver is necessary to perform OTFS detection.

5.1 Separate Pilot Approach

The impulse-based channel estimation technique employs an impulse function, denoted as $\delta(k,l)$, in the DD domain as the pilot signal. Specifically, the pilot is represented by $\delta(k_p,l_p)$. In the allocation scheme, the pilot symbol is denoted as x_p, while the guard symbol is represented as '0'. The pilot corresponding to a specific allocation is allocated as follows:

$$x[k,l] = \begin{cases} x_p & k = k_p, l = l_p, \\ 0 & \text{otherwise.} \end{cases}$$

$$x_p[k,l] = \begin{cases} 1, \text{ if } (k,l) = (k_p,l_p) \\ 0, \forall\ (k,l) \neq (k_p,l_p)\,. \end{cases}$$

The interaction of the pilot with the channel results in a two-dimensional periodic convolution of the DD impulse response with the pilot. The received pilot in the DD domain is given by

$$y_p\left[k',l'\right] = \frac{1}{MN}\tilde{h}\left[\left(k'-k_p\right)_N, \left(l'-l_p\right)_M\right] + v\left[k',l'\right],$$

At the receiver, we employ a threshold-based channel estimation method. The threshold is selected based on the channel characteristics.

5.2 Embedded Pilot Approach

In the preceding section, a complete OTFS frame was utilized for pilot transmission, and the obtained channel information was subsequently employed for data detection in the subsequent frame. However, this approach may prove ineffective if the channel estimation becomes outdated by the time the subsequent frame is processed. In this section we shall look at embedded-pilot OTFS channel estimation.

To ensure minimal interference between pilot and data symbols, we organize a single pilot symbol, guard symbols, and data symbols in the delay-Doppler grid for each OTFS frame. At the receiver, we employ a threshold-based channel estimation method. The threshold is selected based on the channel characteristics and symbol arrangement

to optimize the accuracy of the estimation. Through our carefully designed symbol arrangements, we achieve efficient channel estimation and data detection within the same OTFS frame, resulting in a minimal overhead.

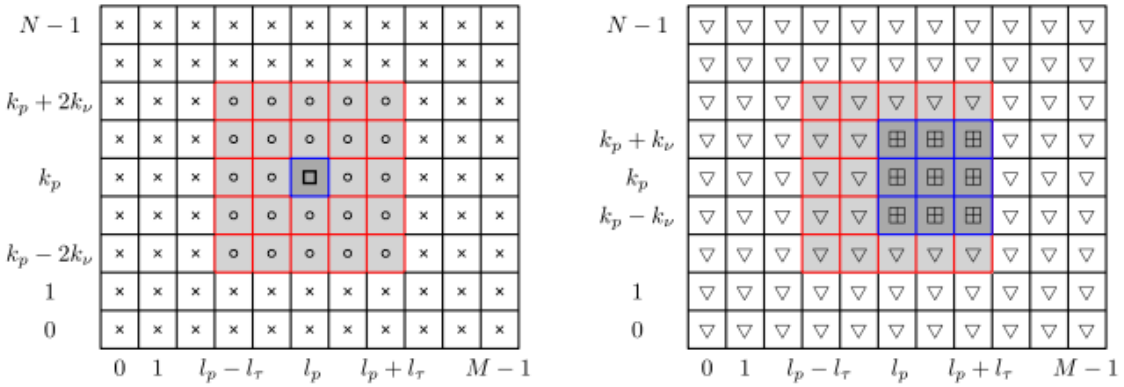

(a) Tx symbol arrangement (□: pilot; ∘: guard symbols; ×: data symbols)

(b) Rx symbol pattern (▽: data detection, ⊞: channel estimation)

Figure 5.1: Embedded Pilot based CE : Transmitted and Received OTFS frame

The pilot symbol is denoted as x_p and has a pilot signal-to-noise ratio (SNR) of $\mathrm{SNR}_p = |x_p|^2/\sigma^2$. The data symbols are represented by x_d with a data SNR of $\mathrm{SNR}_d = \mathbb{E}(|x_d|^2)/\sigma^2$ in the delay-Doppler information grid. We use the symbol '0' to indicate the guard symbol.

In each OTFS frame transmission, we allocate one pilot symbol x_p, N_n guard symbols, and $M(N - N_n - 1)$ information symbols within the delay-Doppler grid Γ. By carefully arranging the symbols, we can separate the received symbols into two distinct groups at the receiver: the first group comprises pilot and guard symbols used for channel estimation, while the second group is utilized for data detection. The presence of guard symbols ensures that the received symbols for channel estimation and data detection do not interfere with each other. This separation facilitates more accurate channel estimation, which is crucial for effective data detection within the same frame.

To determine the location of the pilot symbol, we initially choose an arbitrary grid position $[k_p, l_p]$ satisfying $0 \leq k_p \leq N-1$ and $0 \leq l_p \leq M-1$. For convenience, we define $0 \leq l_p - l_\tau \leq l_p \leq l_p + l_\tau \leq M-1$ and $0 \leq k_p - 2k_\nu \leq k_p \leq k_p + 2k_\nu \leq N-1$, where l_τ and k_ν represent the taps corresponding to the maximum delay and Doppler values, respectively.

In Fig. 5.1a, we illustrate the arrangement of the pilot, guard, and data symbols

within the delay-Doppler grid for an OTFS frame transmission.

At the receiver, we utilize the received symbols $y[k,l]$ within the grid $k_p - k_\nu \leq k \leq k_p + k_\nu, l_p \leq l \leq l_p + l_\tau$ for channel estimation. The remaining received symbols $y[k,l]$ on the grid are used for data detection, as depicted in Fig. 5.1b.

Based on the proposed transmit symbol arrangement, we can express the received symbols for channel estimation as:

$$y[k,l] = b[k-k_p, l-l_p]\hat{h}[k-k_p, l-l_p]x_p + v[k,l]$$

for $k \in [k_p - k_\nu, k_p + k_\nu]$ and $l \in [l_p, l_p + l_\tau]$. Here, if there exists a path with a Doppler tap of $k - k_p$ and a delay tap of $l - l_p$, i.e., $b[k-k_p, l-l_p] = 1$, then we have $y[k,l] = \hat{h}[k-k_p, l-l_p]x_p + v[k,l]$. Otherwise, $y[k,l] = v[k,l]$. Similarly, we can express the received symbols for data detection, illustrating that there is no interference between the received symbols used for channel estimation and those used for data detection.

We propose a straightforward channel estimation algorithm as follows: For $k \in [k_p - k_\nu, k_p + k_\nu]$ and $l \in [l_p, l_p + l_\tau]$, if the magnitude $\|y[k,l]\| \geq \mathcal{T}$, where $\mathcal{T}$ is a positive detection threshold, then we estimate $b[k-k_p, l-l_p] = 1$ and $\hat{h}[k-k_p, l-l_p] = y[k,l]/x_p$. Otherwise, we set $b[k-k_p, l-l_p] = \hat{h}[k-k_p, l-l_p] = 0$. The proposed threshold-based scheme relies on the fact that if a path exists, the received symbol is the scaled pilot signal with additive white Gaussian noise. Otherwise, it is only noise.

5.3 Superimposed Pilot Approach

In this approach, pilot symbols are super-imposed on the data symbols in an OTFS frame. The mutual interference between the pilot and the data symbols are handled by an optimum selection of pilot SNR. The proposed framework does not require a dedicated pilot frame to estimate the channel. The proposed framework will thus have significantly higher spectral efficiency than the previous two methods, with a minor BER degradation, a fact we will numerically validate later.

The SP-aided channel estimation can be performed either non-iteratively or iteratively. Non-iterative SP-aided channel estimation exploits channel sparsity and uses a compressed sensing method to estimate the channel. However, due to interference between pilot and data symbols, the bit error rate (BER) in the pilot frame is poorer than that in the data-only frame (although still much better than embedded-pilot/separate-pilot impulse-based channel estimation). Iterative SP-aided channel estimation mitigates this interference by iterating between channel estimation and data detection in the delay-Doppler domain, and it achieves better BER and spectral efficiency (SE) in the pilot frame as well. However, in this work, we focus only on non-iterative SP-aided channel estimation.

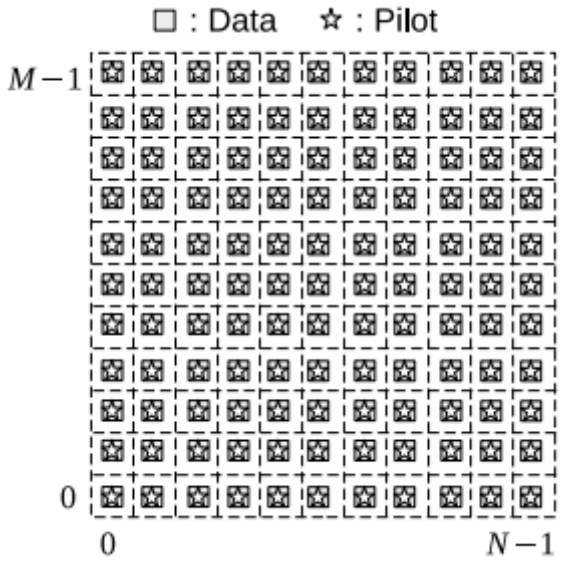

Figure 5.2: Superimposed Pilot Channel Estimation : Transmit frame

Figure 5.2 depicts a typical superimposed-pilot OTFS frame used for channel estimation and data detection. From section 4.5, the input-output relation of the OTFS system in the SP framework can be written as,

$$\mathbf{y} = \left(\sum_{i=1}^{P} h_i \mathbf{\Gamma}_i \right) (\mathbf{x}_p + \mathbf{x}_d) + \tilde{\mathbf{w}}.$$

$$\mathbf{y} = \mathbf{\Omega}_p \mathbf{h} + \mathbf{\Omega}_d \mathbf{h} + \tilde{\mathbf{w}}$$

The concatenated matrices $\mathbf{\Omega}_p \in \mathbb{C}^{MN \times MN}$ and $\mathbf{\Omega}_d \in \mathbb{C}^{MN \times MN}$ corresponding to the pilot vector $\mathbf{x}_p$ and data vector $\mathbf{x}_d$ are obtained as follows

$$\mathbf{\Omega}_p = \begin{bmatrix} \mathbf{\Gamma}_1 \mathbf{x}_p & \mathbf{\Gamma}_2 \mathbf{x}_p & \cdots & \mathbf{\Gamma}_{MN} \mathbf{x}_p \end{bmatrix}$$
$$\mathbf{\Omega}_d = \begin{bmatrix} \mathbf{\Gamma}_1 \mathbf{x}_d & \mathbf{\Gamma}_2 \mathbf{x}_d & \cdots & \mathbf{\Gamma}_{MN} \mathbf{x}_d \end{bmatrix}.$$

We will further look into the channel estimation details of SP-aided channel estimation method after studying the Compressed sensing and its application in channel estimation for sparse channels like delay-Doppler channels.

CHAPTER 6

COMPRESSED SENSING BASED CHANNEL ESTIMATION TECHNIQUES

Next generation communication systems are anticipated to possess intelligence and agility in efficiently sensing the wideband spectrum and identifying available channels. Numerous sensing techniques have been proposed in recent decades, including energy detection, Matched filter, autocorrelation, autocorrelation-based Euclidean distance, and Bayesian inference method. These techniques rely on measurements sampled at the Nyquist rate using an Analog/Digital Converter (ADC), which can lead to significant processing time, hardware cost, and computational complexity. To address these challenges, compressive sensing has emerged as a solution to reduce processing time and expedite the spectrum scanning process.

6.1 A Brief Tutorial on Compressed Sensing

The theory of compressive sensing states that specific signals can be effectively reconstructed using fewer measurements compared to what the Nyquist/Shannon sampling principle requires. Compressive sensing comprises three primary stages: **sparse representation**, **measurement (encoding)**, and **sparse recovery (decoding)**.

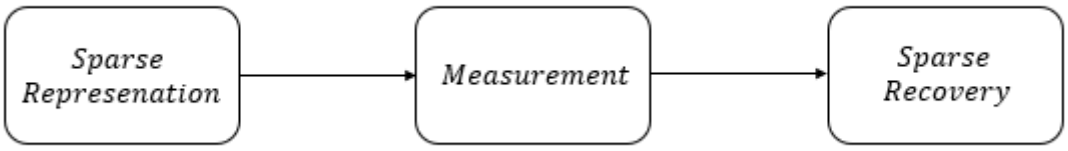

Figure 6.1: Compressive Sensing Processes

Sparse Representation : The initial step, sparse representation, involves expressing the signal through a set of projections on a suitable basis. Sparse representation

techniques such as Wavelet Transform (WT), Fast Fourier Transform (FFT), and Discrete Cosine Transform (DCT) are commonly used examples. A signal x is considered K-sparse if only K elements of its entries are non-zero. Mathematically, this condition can be written as $\sum \|x\|_0 \leq K$, where $\|.\|_0$ is the $L0$- norm and K represents the sparsity level of the signal. In cases where a given signal is not sparse, applying a simple projection onto a suitable basis can render it sparse.

Measurement : The second step, measurement, involves acquiring a small number of measurements (denoted as $y \in R^M$) from the sparse signal ($x \in R^N$). Mathematically, this can be represented as the multiplication of the sparse signal x by a matrix $\phi \in R^{M \times N}$, where the matrix ϕ serves as the measurement matrix. Here, M represents the number of measurements, N represents the length of the sparse signal, and $\mathrm{M} << \mathrm{N}$. During this reduction from R^N to R^M, compression is required to preserve the essential information contained in the K-sparse signal, which is necessary for recovering the original signal from these limited measurements. Measurement matrices can be categorized as random or deterministic matrices. Random matrices have certain drawbacks, such as expensive hardware implementation. Deterministic matrices have been proposed as an alternative to minimize randomness. Examples of deterministic matrices include Toeplitz and Circulant matrices.

Sparse Recovery : The final step, sparse recovery, focuses on reconstructing the sparse signal x from a limited set of measurements y. Typically, the sparse recovery problem involves an underdetermined system of linear equations that requires a sparse prior for solving. Due to the underdetermined nature of this system, the existence and uniqueness of the solution are ensured when the signal is adequately sparse, and the measurement matrix satisfies the Restricted Isometry Property (RIP) at a specific level. While the sparse recovery algorithms can be classified into Convex and Relaxation, Greedy and Bayesian categories, we will focus only on Orthogonal Matched Pursuit algorithm, a greedy solution.

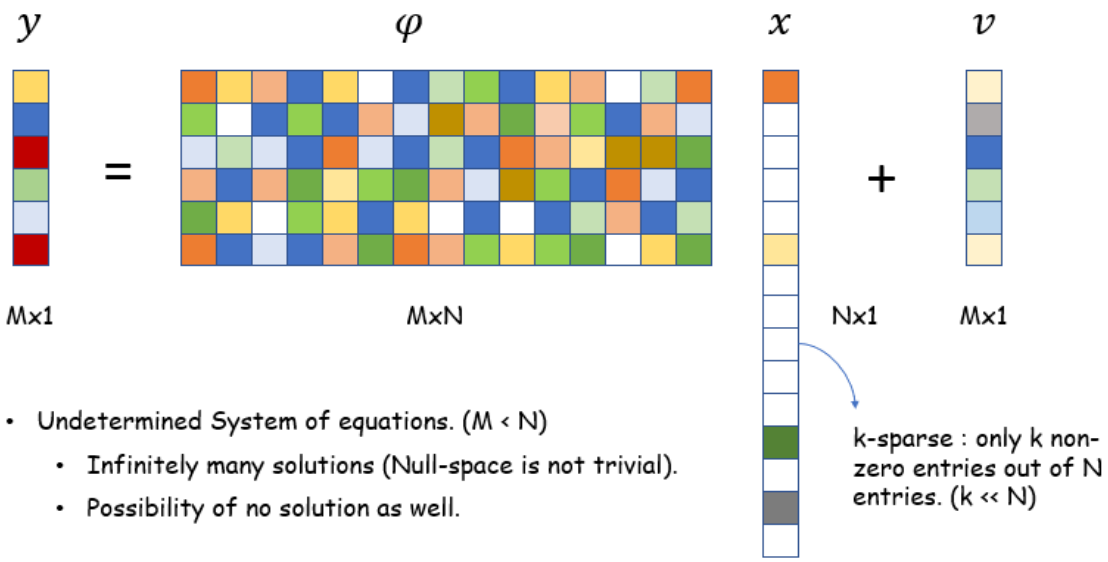

Figure 6.2: Sparse Signal Recovery Problem

The sparse signal recovery problem can be mathematically formulated as follows :

Given y and ϕ -

$$\text{Noiseless Case} : \min\|x\|_0 \quad \text{subject to} \quad y = \phi x$$

$$\text{Noisy Case} : \min\|x\|_0 \quad \text{subject to} \quad \|y - \phi x\|_2 \leq \beta$$

However, solving an $L0$- norm minimization is combinatorially complex (NP-Hard problem), and the theory of compressive sensing has found many approximations to solve this problem. One such approximation is known as basis pursuit (BP) and solves the following convex approximation to

$$\min\|x\|_1 \quad \text{subject to} \quad y = \phi x$$

Figure 6.3 shows how an NP-hard $L0$-norm minimization problem can be approximated

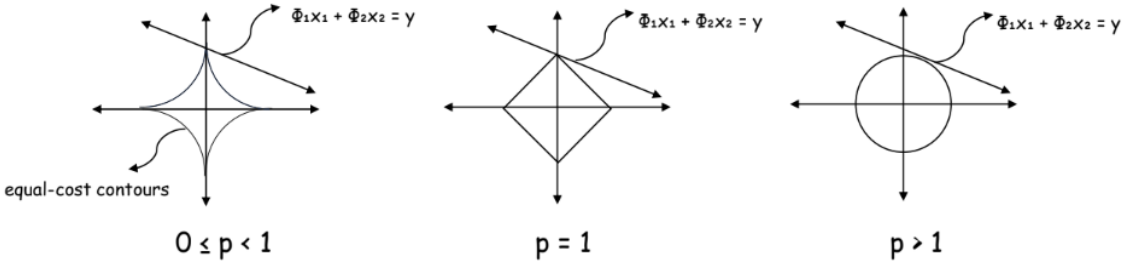

Figure 6.3: Solving a general p-norm optimization subject to a linear constraint

and cast into a $L1$-norm convex optimization problem solvable in polynomial time. The above approximation of the problem is allowed under the condition of Restricted Isometry Property which is discussed in detail in [].We will now look into Orthogonal Matched Pursuit algorithm, a greedy approach to solve the $L1$-norm convex optimization problem.

Orthogonal Matched Pursuit Algorithm :

- An iterative algorithm (it finds x element-by-element in a step-by-step iterative manner).

- A greedy algorithm (at each stage, the problem is solved optimally based on current info).

Algorithm Overview :

- To recover x, given only (y, ϕ) utilize the fact that x is sparse .
- Compute the correlations of y to all the columns of ϕ, and see which column gives the "highest correlation". That column tells which index of x is non-zero (**Matching** part in OMP).
- For k-sparse x with $k > 1$, the same idea applies with one more step: each time when a column in ϕ is extracted, the effect of the extracted column on vector y has to be filtered so that next time the same column will not be extracted again (**orthogonal** part in OMP).

6.2 CS-based OTFS Channel Estimation

In the context of the DD representation, the channel exhibits sparsity, allowing us to employ estimation techniques based on compressive sensing (CS). Taking this into ac-

count, we formulate the DD channel estimation as a sparse recovery problem. To address this, we introduce an algorithm for OTFS (Orthogonal Time Frequency Space) channel estimation based on orthogonal matching pursuit (OMP). Our results demonstrate that the CS-based estimation approaches outperform impulse-based channel estimation in terms of normalized mean squared error (NMSE) and bit error rate (BER) performance.

6.2.1 Separate Pilot Approach

The received vector y can be written as

$$\mathbf{y} = \mathbf{\Omega}_p \mathbf{h} + \tilde{\mathbf{w}}$$

Note that the vector h is sparse with only P non-zeros out of NM entries. This inherent sparsity can be exploited to achieve efficient channel estimation in the DD domain using CS-based algorithms.

The OMP algorithm (Compressed Sensing technique) for OTFS channel estimation is described in Algorithm 1. The algorithm takes the received signal vector $\mathbf{y}$ and the pilot matrix $\mathbf{\Omega}_p$ as inputs. In each iteration k, the residue from the previous iteration $\mathbf{r}^{k-1}$ is projected onto the columns of $\mathbf{\Omega}_p$, and the index of the column with the highest correlation, denoted as T^k, is added to the current support S^k (lines 4 and 5). Next, the non-zero values corresponding to the obtained support are computed using the least squares method (line 6). The residue is then updated (line 7) to remove the effects of the previously updated support, ensuring new support in the next iteration. This process continues until a stopping criterion is satisfied. We use the energy of the residue, with a threshold ϵ, as the stopping criterion. Importantly, the OMP algorithm does not require prior knowledge of the number of paths in the channel. Both the number of paths and the channel's sparsity are determined adaptively during the estimation process. Note if the number of paths is known, then it is enough to run the iteration only those many times as number of taps.

Algorithm 1 OMP-CS based OTFS channel estimation

Initialize: $k = 0$, $h_0 = 0$, $S_0 = \emptyset$, $r_0 = y$
while $\|r_k\|_2 > \epsilon$ **do**
    $k = k + 1$
    $T_k = \arg\max_j |\mathbf{\Omega}_p^H r_{k-1}|$ ▷ Support estimation
    $S_k = S_{k-1} \cup T_k$ ▷ Support update
    $h_{S_k} = \mathbf{\Omega}_{p\,S_k}^{\dagger} y$ ▷ Calculate non-zeros
    $r_k = y - \mathbf{\Omega}_{p\,S_k} h_{S_k}$ ▷ Residue update
end while
Output: Estimated OTFS channel vector $\hat{h}_{S_k} = X_{S_k}^{\dagger} y$ and $\hat{h}_{S_k} = 0$

6.2.2 Superimposed Pilot Approach

We will continue our discussion on SP-aided channel estimation from section 5.3. We will look into how OMP algorithm discussed in 6.2.1 be applied here. The input-output relation of the OTFS system in the SP framework can be written as,

$$\mathbf{y} = \mathbf{\Omega}_p \mathbf{h} + \mathbf{\Omega}_d \mathbf{h} + \tilde{\mathbf{w}}$$

To estimate channel vector $\mathbf{h}$, the data interference is considered as noise. While applying OMP for channel estimation, consider the covariance of the total interfering noise while evaluating the pseudo-inverse $\mathbf{\Omega}_{p\,S_k}^{\dagger}$.

The estimated channel vector $\hat{\mathbf{h}}$ is further used to remove the effect of the pilot from the received signal so that MMSE can be applied to detect the embedded data symbols. Computationally much more efficient MP algorithm can also be used for data detection, but we will stick to the linear-MMSE method of data symbol detection.

CHAPTER 7

SIMULATION RESULTS & FUTURE DIRECTIONS

In this section, we show the simulation results of OMP superimposed pilot channel estimation and compare them against OMP separate pilot channel estimation, impulse-based embedded pilot, and impulse-based separate pilot channel estimation techniques.

To evaluate the estimation performance, the NMSE criterion is considered, which is defined as NMSE $= \|\hat{\mathbf{h}} - \mathbf{h}\|_2^2 / \| \mathbf{h}\|_2^2$. Also, to compare the detection performance, the BER of the proposed method is compared with the ideal CSI and other methods.

For this study, we consider an OTFS system with the number of delay bins $M = 16$, and the Doppler bins $N = 32$ and set the carrier frequency and subcarrier spacing as 4 GHz and 15 KHz, respectively. The system uses a rectangular pulse, and symbols are drawn from the 4-QAM constellation. We assume a static multi-path channel with 6 delay taps and the length of cyclic-prefix to be 6 as well. Figure 4.2 is the channel model that we will adopt. For SI-pilot based channel estimation we allot 75% power for pilot and 25% power for data symbols.

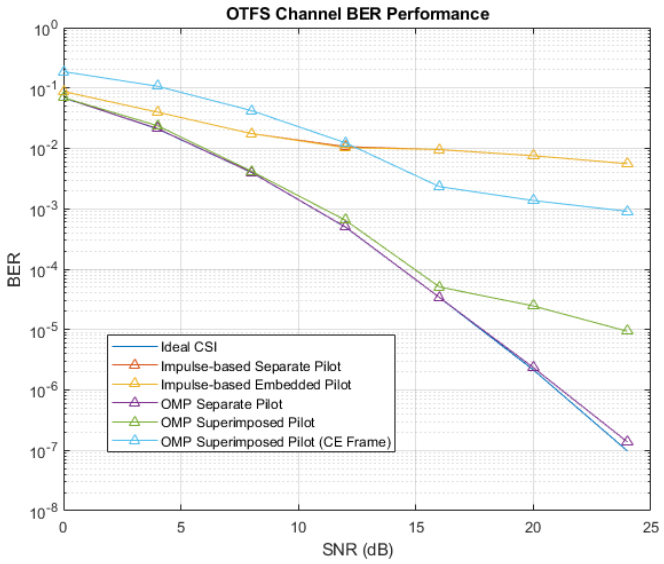

Figure 7.1: OTFS Channel Estimation BER Performance Comparison

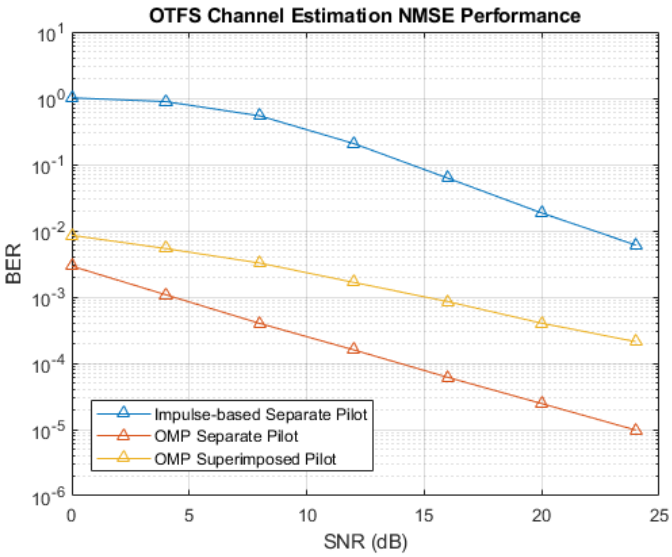

Figure 7.2: OTFS Channel Estimation NMSE Performance Comparison

Figure 7.1 shows the BER comparison between different channel estimation techniques discussed so far. Clearly, OMP (Compressed sensing) based separate pilot (channel estimation with pilot-only frame) channel estimation method gives close to ideal CSI performance.

The BER performance of OMP (Compressed sensing) based superimposed pilot (channel estimation with pilot and data superimposed) channel estimation method gives close to ideal CSI performance for low SNR values and degrades for high SNR. The BER performance for the data symbols in channel estimation frame is poor compared to data-only frame, however its performance beats the conventional impulse-based channel estimation techniques.

Figure 7.2 shows the NMSE performance of the OTFS channel estimation techniques.

7.0.1 Future Direction

OTFS (Orthogonal Time Frequency Space) is an innovative modulation scheme for wireless communications that offers notable performance advantages compared to existing methods. It operates within the delay-Doppler coordinate system, and through our research, we have demonstrated that by utilizing OTFS along with equalization

techniques, all modulated symbols benefit from same channel gain, allowing for optimal extraction of the complete channel diversity.

We have proposed a superimposed pilot-aided OTFS channel estimation, thus not incurring spectral efficiency loss and achieving good BER by exploiting the channel sparsity in the delay-Doppler domain by applying Compressed sensing technique for channel estimation.

The BER performance of OMP SI pilot-based channel estimation can be improved (especially for the Channel Estimation frame) by iterating between channel estimation and data detection, so that the interference between data and pilot symbols can be mitigated thereby improving the data detection accuracy.